Am J Transl Res 2017;9(3):1335-1343
www.ajtr.org /ISSN:1943-8141/AJTR0049851

Original Article

Increased Th9 cells and IL-9 levels accelerate disease progression in experimental atherosclerosis

Qing Li[1*], Tingting Ming[1*], Yuanmin Wang[2], Shaowei Ding[1], Chaojie Hu[1], Cuiping Zhang[1], Qi Cao[3], Yiping Wang[3]

[1]The Central Laboratory of Medical Research Center, Anhui Provincial Hospital, Anhui Medical University, Hefei 230001, Anhui, PR China; [2]Centre for Kidney Research, Children's Hospital at Westmead, Sydney, NSW, Australia; [3]The Centre for Transplantation and Renal Research, Western Clinical School, University of Sydney, Westmead, NSW Australia. [*]Equal contributors.

Received November 24, 2016; Accepted February 24, 2017; Epub March 15, 2017; Published March 30, 2017

Abstract: Atherosclerosis (AS) is the number one killer in developed countries, and currently considered a chronic inflammatory disease. The central role of T cells in the pathogenesis of atherosclerosis is well documented. However, little is known about the newly described T cell subset-Th9 cells and their role in AS pathogenesis. Here, the amounts of Th9 cells as well as their key transcription factors and relevant cytokines during atherosclerosis were assessed in ApoE$^{-/-}$ mice and age-matched C57BL/6J mice. Significantly increased Th9 cell number, Th9 related cytokine (IL-9), and key transcription factor (PU.1) were found in ApoE$^{-/-}$ mice compared with age-matched C57BL/6J mice. Additionally, treatment with rIL-9 accelerated atherosclerotic development, which was attenuated by anti-IL-9 antibodies. These data suggested that both Th9 cells and related IL-9 play key roles in the pathogenesis of atherosclerosis, and antibodies against these antigens offer a novel therapeutic approach in AS treatment.

Keywords: Atherosclerosis, Th9 cells, IL-9, inflammation

Introduction

Atherosclerosis (AS) is a chronic inflammatory disease, whose pathogenesis is greatly influenced by immune mechanisms. Specifically, various immune cells, including T lymphocytes such as CD4$^+$ T-helper cells, play important roles in atherosclerosis [1, 2]. CD4$^+$ T cells can be classified into Th1, Th2 and Th17 subsets based on surface markers, functional characteristics, and specific cytokines, which are used to modulate different immune responses.

AS is a specific state of inflammation, and Th-cell subsets play crucial roles in this process. Th1 cells that promote inflammatory processes have important functions in atherosclerosis and subsequent plaque rupture, while Th2 cells that inhibit immune responses at the tissue level may have anti-atherosclerotic effects [3]. However, the identification of the Th17 T helper cell subset at the beginning of the century challenged this Th1/Th2 paradigm, opening new avenues for dissecting molecular patterns in cellular immunology. Consequently, it was soon demonstrated that Th17 cells and related cytokines, such as IL-17A and IL-6, are also critical in AS pathogenesis [4, 5].

IL-9 was initially considered a growth factor for T cells and mast cells, with pleiotropic functions in the immune system. Multiple cell types, including T cells, natural killer T cells (NKTs) and mast cells, produce IL-9 [6]. Notably, Th9 cells, characterized by high secretion levels of IL-9, are involved in a broad range of autoimmune disorders and allergic inflammation [7, 8]. Dardalhon et al. used IL-4 and TGF-β in combination to polarize CD4$^+$ lymphocytes towards a Th9 phenotype [9].

It has also been reported that Th9 cells and IL-9 are related to the pathogenesis of infectious diseases, cancer immunity, and autoimmune inflammatory disorders [10-12]. Recently, Th9 cells and IL-9 levels were found to be increased in plasma and carotid plaques of patients with carotid and coronary atherosclerosis [13].

However, the mechanism by which Th9 cells influence atherosclerosis pathogenesis remains unclear. The present study assessed whether Th9 cells and IL-9 are involved in atherosclerosis progression in ApoE$^{-/-}$ mice, which exhibit similar atherosclerotic lesion formation as in humans.

Materials and methods

Animal models

To model atherosclerosis *in vivo*, ApoE$^{-/-}$ mice on a C57BL/6J background and C57BL/6 mice were purchased from the Animal Center of Beijing University (Beijing, China). The animals were 8 weeks of age, weighed 20-22 g, and were housed at 24°C in a 12-h/12-h light-dark cycle room in the Anhui Medical University Animal Care Facility, according to institutional guidelines. This study followed the Guide for the Care and Use of Laboratory Animals published by the US National Institutes of Health. All animal experiments were approved by the Animal Care and Utilization Committee of Anhui Medical University. Male ApoE$^{-/-}$ mice were fed high-cholesterol diet (1.3% cholesterol, 0.2% thimecil and 16.2% lard) for 4-24 weeks, starting from 8 weeks of age, to induce atherosclerotic plaque formation, consistent with standard atherosclerotic mouse models. Age-matched C57BL/6J littermates were fed a regular diet as a control group. Mice were fed for 0, 4, 12 and 24 weeks (n=12 per group) before euthanasia and analysis.

ApoE$^{-/-}$ mice were randomly divided at 8 weeks of age into control and intervention groups. Mice were treated with the phosphate buffered saline (PBS), recombinant IL-9 (rIL-9) and anti-mouse IL-9 mAb (IL-9 Ab) respectively via tail vein injection (n=5 each group). Treatments included 100 μg anti-mouse IL-9 mAb (R&D Systems, USA) dissolved in 0.2 ml PBS containing 1% BSA, and 0.2 ml PBS containing 1% BSA or 200 ng rIL-9 (eBioscience, USA) for 12 weeks, respectively.

Serum lipid and lipoprotein profiling

Total serum cholesterol, triglyceride (TG), and high-density lipoprotein (HDL) levels were determined by enzymatic methods. The assays were conducted on an Olympus AU2700 biochemical auto-analyzer (Olympus, Japan).

Histological analysis and evaluation of atherosclerotic lesions

Mice aorta specimens were fixed in 10% neutral-buffered formalin and subsequently embedded in paraffin. Then, 4 μm sections of the paraffin block were stained with periodic acid-Schiff reagent, counterstained with hematoxylin using a standard protocol, and analyzed by light microscopy. The average plaque area (percentage of total area) was determined with Image-Pro Plus 6.0 (Media Cybernetics). Quantification of lesion areas was performed by a single observer blinded to the experimental protocol. Images were acquired and analyzed with a computer image analysis software.

Cell preparation and flow cytometry

Fresh spleens removed from mice were gently squeezed with sterile needles in cold PBS, and passed through stainless steel mesh screens, to yield single-cell suspensions. Splenic lymphocytes were isolated by Ficoll-Hypaque and resuspended in RPMI 1640 (Gibco, USA); cell viability detected by trypan blue staining was >95%.

To assess Th9 cells, splenocytes were resuspended at a density of 2×10^6 cells/ml in complete culture medium (RPMI 1640 supplemented with 100 U/ml penicillin, 100 μg/ml streptomycin, 2 mM glutamine and 10% heat-inactivated fetal calf serum, Gibco BRL). The cell suspension was transferred into 24-well plates, and stimulated with phorbol myristate acetate (PMA, 25 ng/ml) plus ionomycin (1 μg/ml) for 5 h, in the presence of monensin (1.7 μg/ml, Alexis Biochemicals, San Diego, CA). The cells were incubated at 37°C in a 5% CO_2 environment, and collected by centrifugation at 1200 rpm for 5 min.

Next, cells were incubated with fluorescein isothiocyanate (FITC)-conjugated anti-CD4 (RM4-5 clone, eBioscience, USA) for 20 minutes at room temperature in the dark, followed by a PBS wash. Cells were then fixed and permeabilized with the Fix/Perm reagent (Beckman Coulter-Immunotech) according to the manufacturer's instructions, incubated with phycoerythrin (PE)-conjugated anti-IL-9 (RM9A4 clone, eBioscience) or its isotype control antibody. After washing with PBS, the cells were analyzed by FCM on a FACS Aria II flow cytome-

Table 1. Body weights and plasma lipid levels

Feeding time (weeks)	Mice	Weight (g)	TC (mmol/L)	TG (mmol/L)	HDL-C (mmol/L)
0W	C57BL/6J	22.37±0.58	2.89±0.43	0.78±0.21	1.42±0.21
	ApoE$^{-/-}$	23.71±0.94	9.95±1.45◆	1.05±0.18	1.03±0.11*
4W	C57BL/6J	23.19±1.25	2.92±0.84	1.12±0.24	1.28±0.19
	ApoE$^{-/-}$	25.96±1.47	15.51±2.03◆	1.34±0.27	0.89±0.15*
12W	C57BL/6J	26.43±2.58	3.01±0.79	0.98±0.23	1.53±0.24
	ApoE$^{-/-}$	28.94±3.69	26.31±2.48◆	1.62±0.31*	0.73±0.12◆
24W	C57BL/6J	29.08±2.87	2.86±0.75	1.09±0.27	1.37±0.28
	ApoE$^{-/-}$	31.17±3.32	30.29±3.15◆	2.33±0.36*	0.58±0.17◆

Values are expressed as mean ± SD. TC, total cholesterol; TG, triglycerides; HDL-C, high-density lipoprotein cholesterol. *P<0.05 vs. age-matched C57BL/6J littermates; ◆P<0.01 vs. age-matched C57BL/6J littermates.

ter with the BD FACSDiva software (Becton Dickinson, San Jose, CA, USA). The rates of Th9 ($CD4^+IL\text{-}9^+$) cells were expressed as percentage of $CD4^+$ T cells by sequential gating of lymphocytes and $CD4^+$ T cells.

Real-time PCR

Spleens and aortas were removed quickly after perfusion with PBS. Thoracic and abdominal aortas were snap-frozen in liquid nitrogen for later RNA extraction. Total RNA was extracted from the spleens and aortic arches using TRIzol Reagent (Invitrogen, USA) according to the manufacturer's instructions, and reverse transcription was performed with RNA PCR Kit (Invitrogen, USA). RNA amounts and purity were determined by optical density (OD) measurements at 260 and 280 nm. First strand cDNA for qPCR analysis was then synthesized using random hexamer primers and RNase H-reverse transcriptase (Invitrogen). Gene expression levels of PU.1 were determined with SYBR Green Master Mix (Takara, Japan) on an ABI Prism 7500 sequence Detection System (Applied Biosystems, USA). Each sample was analyzed in duplicate and normalized to the house keeping gene GAPDH.

The primers used were: PU.1, F 5'-GCATCTGGTGGGTGGACAA-3' and R 5'-TCTTGCCGTAGTTGCGCAG-3'; GAPDH, F, 5'-TAAGAGACAGCCGCATCT-3' and R 5'-CGACCTTCACCATTTTGTCTACA-3'.

Levels of cytokines and ox-LDL in serum

Serum IL-9 and ox-LDL levels were assessed by ELISA, measured at 450 nm on a Biocell HT1 ELISA microplate reader (TSZ Company, Minneapolis, USA). Minimal detectable concentrations were 15 pg/ml for IL-9 and 10 μg/L for ox-LDL. Intra- and inter-assay coefficients of variation for all ELISAs were <5%. Samples were measured in duplicate.

Statistical analyses

Values are mean ± standard deviation (SD), and were analysed by the SPSS software (Version 13.0; SPSS, Chicago, IL, USA). Groups were compared by 2-tailed Student *t*-test or one-way analysis of variance (ANOVA). Bonferroni's test was performed for post-hoc analysis to detect differences among groups with assumed equal variance; Dunnett's C test was carried out when equal variance was not assumed. Spearman's correlation was used to determine correlations between two continuous variables. P<0.05 was considered statistically significant.

Results

Body weights and plasma lipid levels are increased in ApoE$^{-/-}$ mice

Body weights and serum cholesterol levels are shown in **Table 1** for ApoE$^{-/-}$ mice fed a high-cholesterol diet and C57BL/6J mice fed a regular diet over a 24-week period.

Atherosclerotic lesion size is significantly increased in ApoE$^{-/-}$ mice

ApoE$^{-/-}$ mice showed overt atherosclerotic lesions with progressive development, whereas only few C57BL/6J mice had such lesions (**Figure 1**). Increased thickness of arterial internal membrane was detectable after 4 weeks of feeding. Atherosclerotic lesion sizes steadily increased significantly from weeks 12 to 24 of

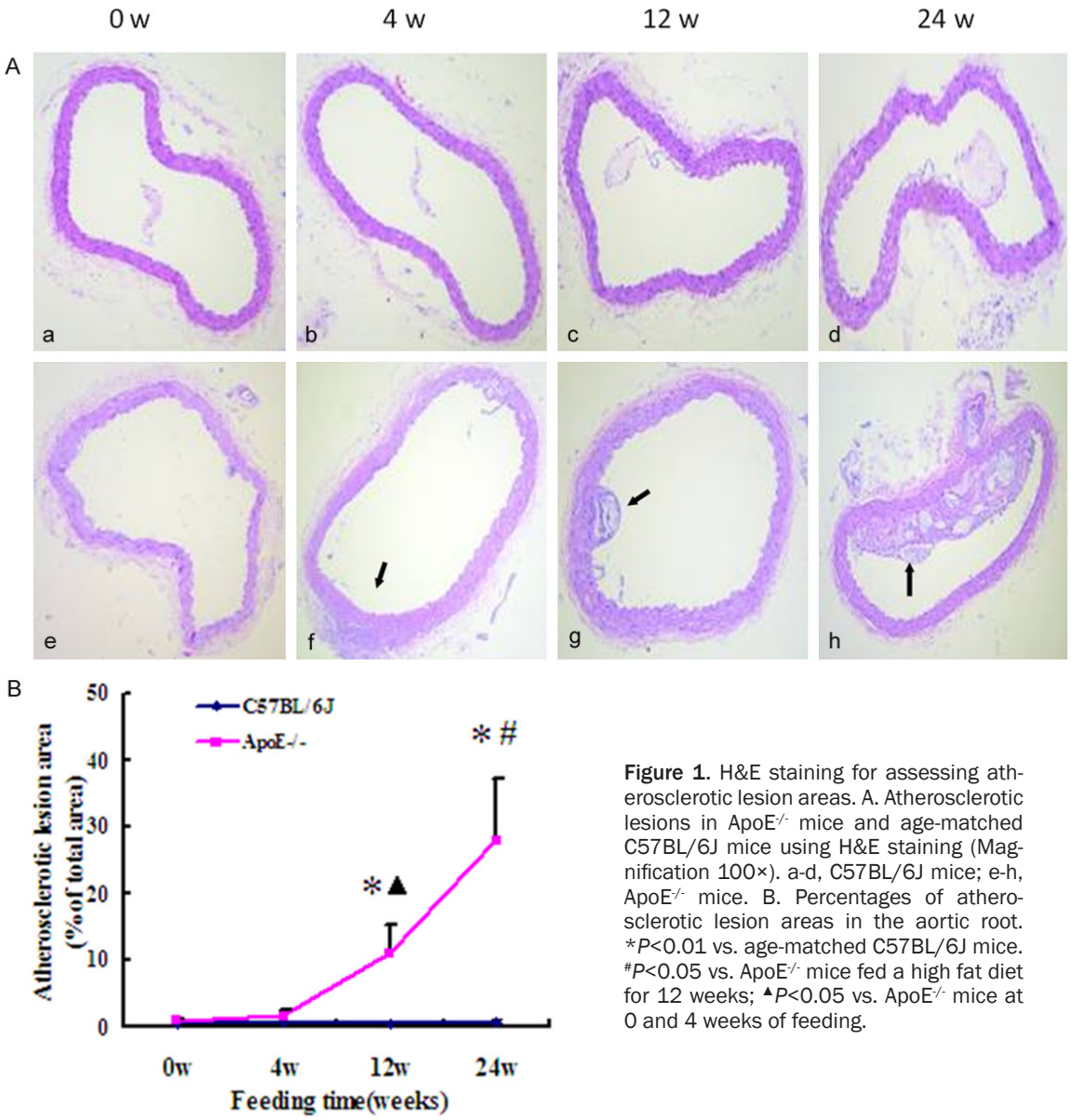

Figure 1. H&E staining for assessing atherosclerotic lesion areas. A. Atherosclerotic lesions in ApoE$^{-/-}$ mice and age-matched C57BL/6J mice using H&E staining (Magnification 100×). a-d, C57BL/6J mice; e-h, ApoE$^{-/-}$ mice. B. Percentages of atherosclerotic lesion areas in the aortic root. *P<0.01 vs. age-matched C57BL/6J mice. $^{\#}P$<0.05 vs. ApoE$^{-/-}$ mice fed a high fat diet for 12 weeks; $^{\blacktriangle}P$<0.05 vs. ApoE$^{-/-}$ mice at 0 and 4 weeks of feeding.

feeding, compared with earlier time points (P<0.05).

Rates of Th9 cells are increased in spleens from ApoE$^{-/-}$ mice fed a high-fat diet

Flow cytometry was used to assess Th9 cells in C57BL/6J and ApoE$^{-/-}$ mice. Spleen cells from 12 mice per group were obtained at each time point. Interestingly, the Th9 cell rate was positively correlated with feeding duration, and peaked at feeding week 24 in ApoE$^{-/-}$ mice fed a high-fat diet (**Figure 2A**). However, significant differences in Th9 cell amounts were observed in ApoE$^{-/-}$ mice between feeding weeks 12 and 24 (P<0.01). Additionally, Th9 cell amounts in ApoE$^{-/-}$ mice were prominently increased compared with those of C57BL/6J mice at feeding week 4. Furthermore, Th9 cell rates were markedly elevated in ApoE$^{-/-}$ mice fed a high-fat diet compared with the values of age-matched C57BL/6J counterparts starting from feeding week 4 (**Figure 2B**, P<0.01).

Increased levels of Th9-related-transcription factors in spleens and aortas of ApoE$^{-/-}$ mice

As shown in **Figure 3A**, PU.1 expression levels in the spleen were significantly higher in ApoE$^{-/-}$ mice fed a high-fat diet than their age-matched C57BL/6J littermates at the 4-24 week feeding time points (all P<0.01). Furthermore, ApoE$^{-/-}$

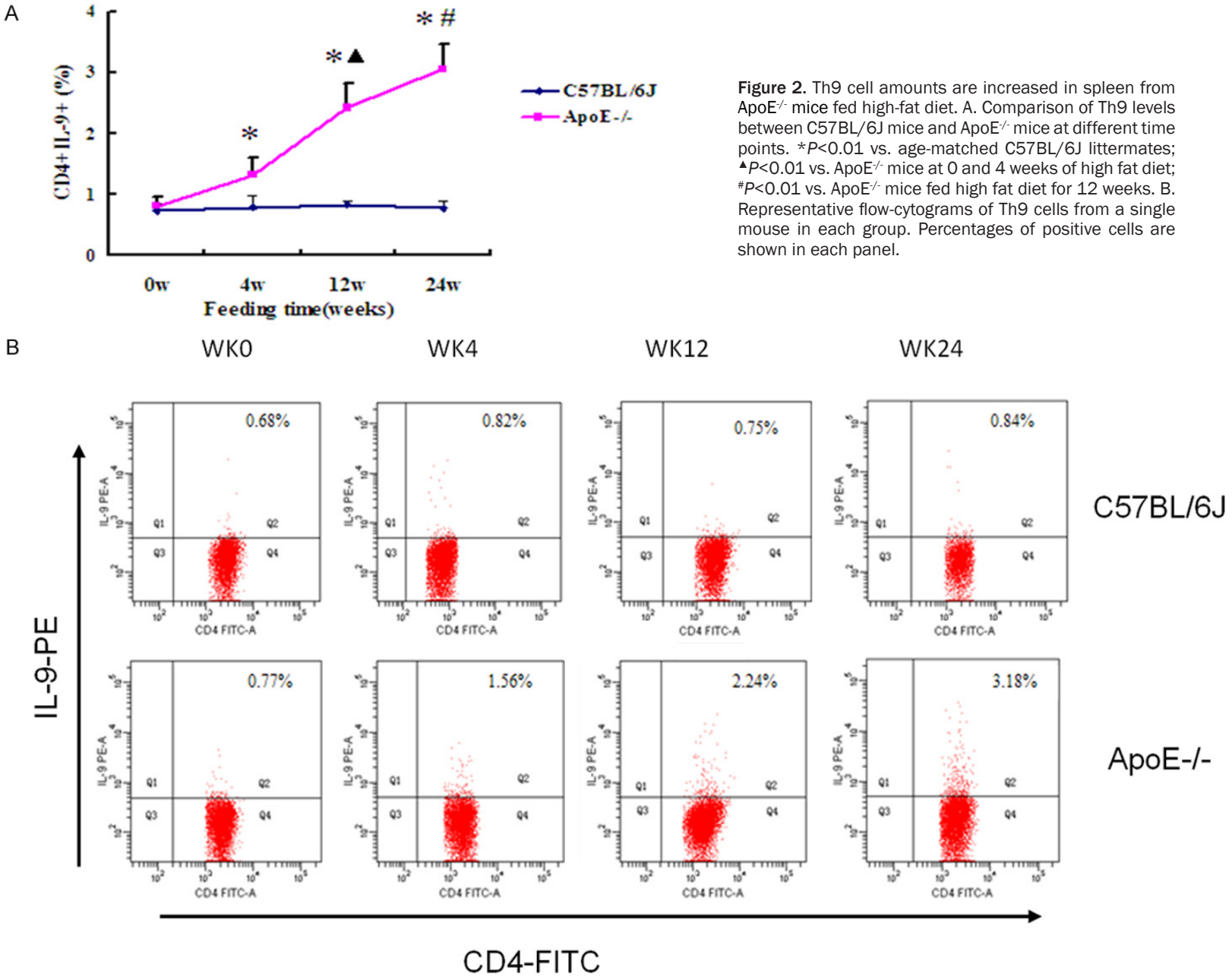

Figure 2. Th9 cell amounts are increased in spleen from ApoE$^{-/-}$ mice fed high-fat diet. A. Comparison of Th9 levels between C57BL/6J mice and ApoE$^{-/-}$ mice at different time points. *P<0.01 vs. age-matched C57BL/6J littermates; ▲P<0.01 vs. ApoE$^{-/-}$ mice at 0 and 4 weeks of high fat diet; #P<0.01 vs. ApoE$^{-/-}$ mice fed high fat diet for 12 weeks. B. Representative flow-cytograms of Th9 cells from a single mouse in each group. Percentages of positive cells are shown in each panel.

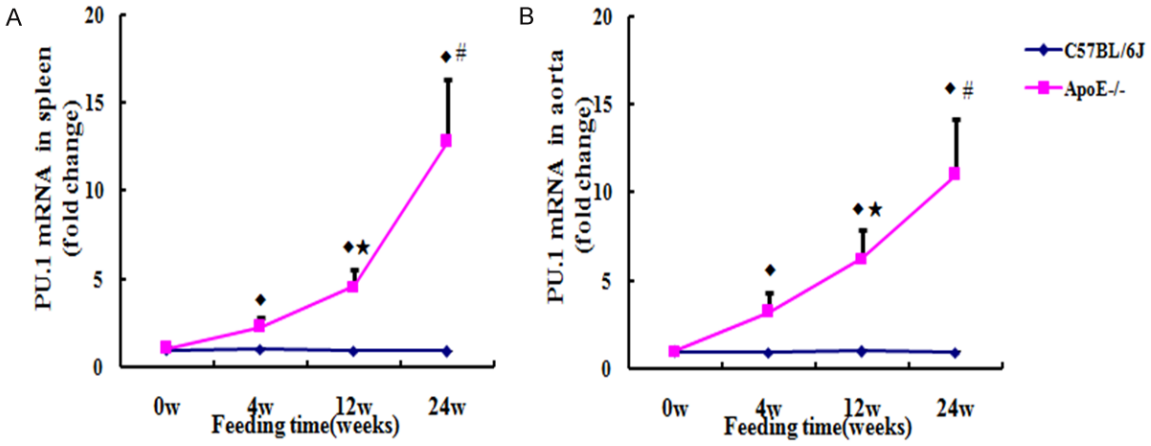

Figure 3. Increased levels of Th9-related-transcription factors in the spleen and aorta of ApoE$^{-/-}$ mice. Gene expression levels of Th9 in the spleen (A) and aorta (B). ◆P<0.01 vs. age-matched C57BL/6J littermates; ★P<0.01 vs. ApoE$^{-/-}$ mice at 0-4 weeks of high fat diet; #P<0.01 vs. 12 weeks of feeding time.

Table 2. Serum IL-9 and ox-LDL levels

Feeding week	Mice	IL-9 (pg/ml)	Ox-LDL (μg/L)
0	C57BL/6J	121.76±25.23	246.75±26.25
	ApoE$^{-/-}$	130.92±28.25	278.89±38.73
4	C57BL/6J	123.57±27.34	247.48±29.12
	ApoE$^{-/-}$	161.27±32.54*	364.75±57.70◆
12	C57BL/6J	118.43±30.12	249.23±35.34
	ApoE$^{-/-}$	191.41±34.40◆	413.66±79.94◆
24	C57BL/6J	124.64±38.43	251.09±32.51
	ApoE$^{-/-}$	221.67±45.73◆,★	439.79±87.86◆

Values are expressed as mean ± SD. *P<0.05 vs. age-matched C57BL/6J littermates; ◆P<0.01 vs. age-matched C57BL/6J littermates; ★P<0.05 vs. ApoE$^{-/-}$ mice fed a high fat diet for 12 weeks.

mice achieved maximal PU.1 expression at the latest time point (feeding week 24). Interestingly, significant differences in PU.1 levels were found in ApoE$^{-/-}$ mice between feeding weeks 12 and 24 (P<0.01).

Next, to examine the involvement of Th9-related-transcription factors in atherosclerosis, we assessed PU.1 levels in aortic arches. As shown in **Figure 3B**, PU.1 levels in aortic arches from ApoE$^{-/-}$ mice were higher than those of age-matched C57BL/6J mice (P<0.01). RT-PCR demonstrated distinct levels of PU.1 expression in early and advanced plaques (**Figure 3B**).

Serum IL-9 and ox-LDL levels are significantly higher in ApoE$^{-/-}$ mice

IL-9 concentrations in ApoE$^{-/-}$ mice fed a high-fat diet were significantly higher compared with those of age-matched C57BL/6J mice (**Table 2**). Furthermore, IL-9 amounts peaked at later age in these mice (24 weeks of feeding). IL-9 levels were significantly different at the different time points in ApoE$^{-/-}$ mice (P<0.05, P<0.01).

Similarly, ox-LDL levels in ApoE$^{-/-}$ mice were higher than those of age-matched C57BL/6J mice at all time points. Ox-LDL levels were positively correlated with prolonged feeding in ApoE$^{-/-}$ mice.

Serum ox-LDL level is positively correlated with Th9 cell rate

Our results showed that serum ox-LDL concentrations were positively correlated with the rate of Th9 cells (P<0.01 and r=0.817). Furthermore, a positive correlation was also found between serum ox-LDL and IL-9 amounts (P<0.01 and r=0.847, **Figure 4**).

Effects of rIL-9 and anti-IL-9 in atherosclerosis

To further explore the role of IL-9 in the development of atherosclerosis, ApoE$^{-/-}$ mice fed a high-fat diet were treated with recombinant IL-9 or monoclonal antibody targeting IL-9 (IL-9 mAb) for 12 weeks. Interestingly, rIL-9 administration led to significantly elevated serum IL-9 levels (424.50+85.67 pg/mL vs. 191.41±38.90 pg/mL, P<0.01) while treatment with IL-9 mAb reduced serum IL-9 levels (56.30+10.67 pg/mL vs. 191.41±38.90 pg/mL, P<0.01), compared with the PBS group.

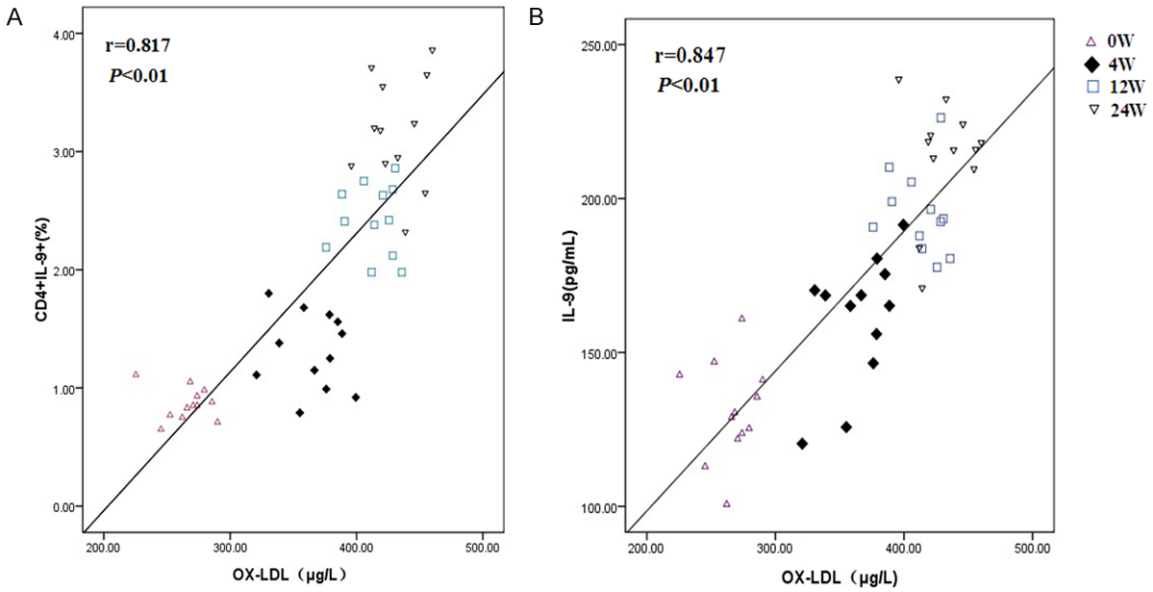

Figure 4. Correlation of serum ox-LDL levels with Th9 cell (A) and IL-9 (B) amounts.

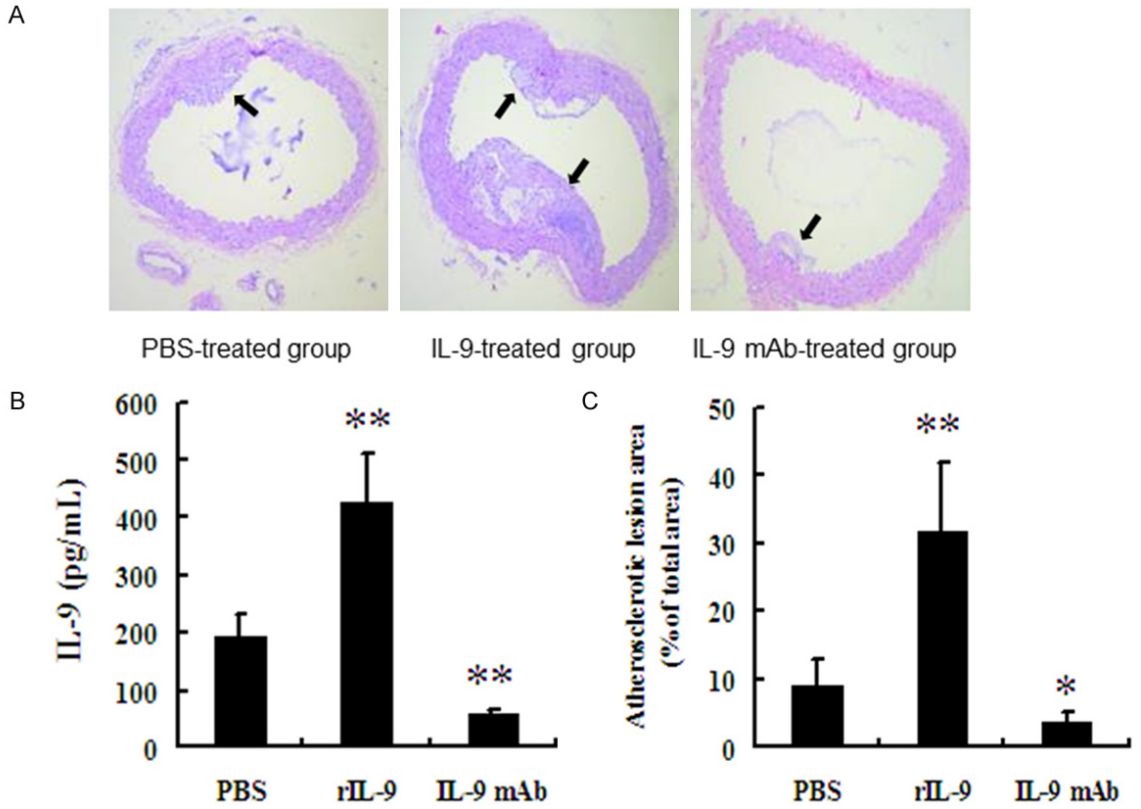

Figure 5. Atherosclerotic lesion areas are significantly increased in mice treated with rIL-9. A. Representative micrographs of H&E staining of aorta samples (Magnification 100×). B. Quantification of aortic lesion areas as percentage of total aortic areas in various groups. C. Serum IL-9 levels in various groups. **P*<0.05 vs. PBS-treatment group; ***P*<0.01 vs. PBS and IL-9 mAb-treatment groups.

Atherosclerotic lesion areas were also significantly increased in mice treated with rIL-9 compared with the PBS and IL-9 mAb treatment groups, respectively (3.89+1.34% vs. 8.94+

3.27%, $P<0.05$). In contrast, atherosclerotic lesions were significantly decreased in size in mice treated with rIL-9 compared with the PBS group (32.18+12.93% vs. 8.94+3.27%, $P<0.01$, **Figure 5**).

Discussion

Th9 cells appeared to have a distinct influence upon the inflammatory processes, playing an important role in the pathogenesis of atherosclerosis. We compared Th9 cell amounts and function between ApoE$^{-/-}$ mice fed a high-fat diet and age-matched C57BL/6J littermates. Significantly increased Th9 rates were found in ApoE$^{-/-}$ mice fed a high-fat diet, as well as higher amounts of the related cytokine IL-9 and key transcription factor (PU.1), compared with age-matched C57BL/6J wild type counterparts. These findings suggested that increased Th9 cell count could play a pathogenic role in the formation and progression of atherosclerosis.

Atherosclerosis is the leading cause of cardiovascular diseases worldwide. It is currently considered a chronic inflammatory disease with progression from fatty streaks to more complex lesions and plaque rupture, which involves a complicated interplay between many immune cell types and cytokine networks. Both innate and adaptive immune responses have been shown to regulate local and systemic inflammation in atherosclerosis [10, 11]. Recently, T cells in AS were shown to be skewed toward a pro-inflammatory phenotype that promotes chronic inflammation through increased pro-inflammatory cytokine production [14].

Th9 cells activate macrophages through IL-9 secretion, leading to the formation and development of atherosclerotic lesions. A genetic deficiency of the transcription factor PU.1, which is critical for Th9 differentiation and IL-9 secretion, leads to reduced prevalence of atherosclerotic lesions in patients with acute coronary syndrome [15]. It was also reported that IL-9 exerts pro-atherosclerotic effects in ApoE$^{-/-}$ mice [16]. Consistently, both systemic and local IL-9 levels are elevated in patients with carotid and coronary atherosclerosis [13, 17]. However, IL-9 can be produced by a variety of other cell types besides Th9 cells.

As shown above, Th9 cell amounts were elevated in early stages, peaking at later stages. This indicated that Th9 cell alteration occurred throughout the whole development of atherosclerotic lesions, potentially contributing to immune activation and inflammation. Increased levels of Th9 cells were definitively correlated with increased number of atherosclerotic lesions in ApoE$^{-/-}$ mice fed a high-fat diet. However, whether Th9 cell alteration is just a consequence of AS or contributes to its initial development remains uncertain, and requires further clarification.

Another important finding of this study is that serum ox-LDL concentrations were positively correlated with Th9 cell and IL-9 levels. Ox-LDL plays an important role in promoting atherosclerosis initiation and progression, along with plaque destabilization [18]. Indeed, circulating ox-LDL amounts reflect the level of oxidative-induced endothelial damage and foam cell formation rate [19]. This further suggests that Th9 cells could play a key role in the pathogenesis of atherosclerosis.

Studies have shown that levels of pro-inflammatory cytokines, including IFN-γ, IL-12, IL-15, IL-18 and TNF, are elevated in AS [20]. In this study, we assessed IL-9 expression, and found that rIL-9 administration markedly increased plaque size, indicating a pathogenic role for IL-9 in atherosclerotic plaque formation. This is consistent with findings by Zhang *et al* [16] that IL-9 aggravates the development of atherosclerosis in ApoE$^{-/-}$ mice. As shown above, blocking IL-9 with specific antibodies resulted in a dramatic reduction of plaque size, further confirming the pathogenic role of IL-9.

In conclusion, Th9 cell amounts, along with IL-9 and PU.1 levels were significantly elevated in AS. Administration of rIL-9 markedly increased plaque size, which was dramatically reduced by treatment with IL-9 mAb, indicating that Th9 cells and IL-9 play a pathogenic role in atherosclerosis. Consequently, antibodies targeting Th9 cells and/or IL-9 may provide a novel approach for AS treatment.

Acknowledgements

This study was supported by the National Natural Science Foundation of China (No. 81472018) and the Natural Science Foundation of Anhui province of China (No. 1408085MH-145, 1508085QH170). We thank Mr. Hamish Wan for assistance in editing the manuscript.

Disclosure of conflict of interest

None.

Address correspondence to: Dr. Qing Li, The Central Laboratory of Medical Research Center, Anhui Provincial Hospital, Anhui Medical University, Hefei 230001, PR China. E-mail: liqing-2001@163.com

References

[1] Binder CJ, Chang MK, Shaw PX, Miller YI, Hartvigsen K, Dewan A, Witztum JL. Innate and acquired immunity in atherogenesis. Nat Med 2002; 8: 1218-1226.

[2] Hansson GK, Libby P. The immune response in atherosclerosis: a double-edged sword. Nat Rev Immunol 2006; 6: 508-519.

[3] Cheng X, Liao YH, Ge H, Li B, Zhang J, Yuan J, Wang M, Liu Y, Guo Z, Chen J, Zhang J, Zhang L. TH1/TH2 functional imbalance after acute myocardial infarction: coronary arterial inflammation or myocardial inflammation. J Clin Immunol 2005; 25: 246-253.

[4] Xie JJ, Wang J, Tang TT, Chen J, Gao XL, Yuan J, Zhou ZH, Liao MY, Yao R, Yu X, Wang D, Cheng Y, Liao YH, Cheng X. The Th17/Treg functional imbalance during atherogenesis in ApoE(-/-) mice. Cytokine 2010; 49: 185-193.

[5] Li Q, Wang Y, Chen K, Zhou Q, Wei W, Wang Y, Wang Y. The role of oxidized low-density lipoprotein in breaking peripheral Th17/Treg balance in patients with acute coronary syndrome. Biochem Biophys Res Commun 2010; 394: 836-842.

[6] Noelle RJ, Nowak EC. Cellular sources and immune functions of interleukin-9. Nat Rev Immunol 2010; 10: 683-687.

[7] Li H, Nourbakhsh B, Cullimore M, Zhang GX, Rostami A. IL-9 is important for T-cell activation and differentiation in autoimmune inflammation of the central nervous system. Eur J Immunol 2011; 41: 2197-2206.

[8] Kara EE, Comerford I, Bastow CR, Fenix KA, Litchfield W, Handel TM, McColl SR. Distinct chemokine receptor axes regulate Th9 cell trafficking to allergic and autoimmune inflammatory sites. J Immunol 2013; 191: 1110-1117.

[9] Dardalhon V, Awasthi A, Kwon H, Galileos G, Gao W, Sobel RA, Mitsdoerffer M, Strom TB, Elyaman W, Ho IC, Khoury S, Oukka M, Kuchroo VK. IL-4 inhibits TGF-beta-induced Foxp3+ T cells and, together with TGF-beta, generates IL-9+ IL-10+ Foxp3(-) effector T cells. Nat Immunol 2008; 9: 1347-1355.

[10] Pilette C, Ouadrhiri Y, Van Snick J, Renauld JC, Staquet P, Vaerman JP, Sibille Y. IL-9 inhibits oxidative burst and TNF-alpha release in lipopolysaccharide-stimulated human monocytes through TGF-beta. J Immunol 2002; 168: 4103-4111.

[11] Purwar R, Schlapbach C, Xiao S, Kang HS, Elyaman W, Jiang X, Jetten AM, Khoury SJ, Fuhlbrigge RC, Kuchroo VK, Clark RA, Kupper TS. Robust tumor immunity to melanoma mediated by interleukin-9-producing T cells. Nat Med 2012; 18: 1248-1253.

[12] Li H, Nourbakhsh B, Ciric B, Zhang GX, Rostami A. Neutralization of IL-9 ameliorates experimental autoimmune encephalomyelitis by decreasing the effector T cell population. J Immunol 2010; 185: 4095-4100.

[13] Gregersen I, Skjelland M, Holm S, Holven KB, Krogh-Sørensen K, Russell D, Askevold ET, Dahl CP, Ørn S, Gullestad L, Mollnes TE, Ueland T, Aukrust P, Halvorsen B. Increased systemic and local interleukin 9 levels in patients with carotid and coronary atherosclerosis. PLoS One 2013; 8: e72769.

[14] Meng K ZQ, Lu Q, Lin Y, Wu B, Yu K, Dong Z, Zhang J, Chai M, Liu Y, Ji Q, Zhou Y. Valsartan attenuates atherosclerosis via up-regulating the Th2 imm une response in prolonged angiotensin II-treated ApoE$^{-/-}$ mice. Mol Med 2015; 21: 143-153.

[15] Lin YZ, Wu BW, Lu ZD, Huang Y, Shi Y, Liu H, Liu L, Zeng QT, Wang X, Ji QW. Circulating Th22 and Th9 levels in patients with acute coronary syndrome. Mediators Inflamm 2013; 2013: 635672.

[16] Zhang W TT, Nie D, Wen S, Jia C, Zhu Z, Xia N, Nie S, Zhou S, Jiao J, Dong W, Lv B, Xu T, Sun B, Lu Y, Li Y, Cheng L. IL-9 aggravates the development of atherosclerosis in ApoE$^{-/-}$ mice. Cardiovasc Res 2015; 106: 453-464.

[17] Taleb S, Tedgui A. IL-9: a new culprit in atherosclerosis? Cardiovasc Res 2015; 106: 348-350.

[18] Hashmi S, Zeng QT. Role of interleukin-17 and interleukin-17-induced cytokines interleukin-6 and interleukin-8 in unstable coronary artery disease. Coron Artery Dis 2006; 17: 699-706.

[19] Cheng X, Yu X, Ding YJ, Fu QQ, Xie JJ, Tang TT, Yao R, Chen Y, Liao YH. The Th17/Treg imbalance in patients with acute coronary syndrome. Clin Immunol 2008; 127: 89-97.

[20] Ilhan F, Kalkanli ST. Atherosclerosis and the role of immune cells. World J Clin Cases 2015; 3: 345-352.